Detection of Two-Quantum Nuclear Coherence by Nuclear Quadrupole Induced Electric Polarization

David C. Newitt[1] and Erwin L. Hahn

Physics Department
University of California
Berkeley, California, 94720

Contents

I. Introduction

The Nobel Prize in Chemistry for 1991 was conferred upon Richard Ernst for his development of elegant NMR techniques and fundamental theory applicable to various types of physical and chemical analysis. These include in particular specific innovations and extensions of pulse Fourier transform methods for NMR high resolution spectroscopy and MRI. We of the NMR community especially salute and congratulate Ernst because the Prize brings honor as well upon all of us who have had so much fun in a field that has yielded many innovations over a time period much longer than many of us expected. The field of NMR in its development reached a stage where one could hardly distinguish whether chemists or physicists were doing NMR. Now the chemists, or rather the physical chemists and biologists, have taken over the field of NMR, and they are doing most of the "physics" nowadays. As a consequence, because chemical technology is more "up front" in the public and commercial eye, people know more about NMR than ever before. Also MRI has had an impact upon the public in the medical and health world, and in scientific research the analytic techniques made possible by NMR have been applied in one form or another to investigations in many disciplines.

In contrast to the utilitarian revelations of the works of Richard Ernst, the authors of this article present in his honor the results of an experiment of the opposite sort, which they hope is acceptable, because most likely the reader will not find our experiment particularly useful. As will be seen in what follows, the electric resonance detection experiment is an interesting exercise in proving that nature will yield the reciprocal of a given effect if one goes to the trouble to expose it. In the course of interpreting such experiments one is forced to improve his understanding of things he thought he understood but in fact did not.

II. Nuclear Electric Resonance Detection

Magnetic one-quantum signal detection of the evolution of multiquantum nuclear spin coherence

[1]Present address: MRSC, Department of Radiology, UCSF, San Francisco, California 94143

always requires the transfer of multiquantum superposition states into one-quantum superposition states (1). A directly observed two-quantum nuclear electric quadrupole radiation signal is conceivable theoretically but beyond observation experimentally (2), since it would be of the order of 10^{-9} the size of an average NMR signal. In this gedanken experiment one would place the sample in a quadrupole capacitor to detect the direct two-quantum nuclear quadrupole radiation signal. However, for nuclear quadrupole moments located at noncentrosymmetric crystal sites, as in the case of As and Ga in GaAs, net local electric-dipole moments are induced in neighboring atoms by the electric quadrupole field of the nucleus. In this report we assume the "stick and ball model" (3). The electric field due to the nuclear quadrupole falls off as r^{-4}, where r is the distance between the point nuclear quadrupole and the point neighboring polarizable atom. The summation of quadrupole induced dipole moments over the set of nearest-neighbor atoms and over the spin ensemble yields a detectable macroscopic polarization. The polarizability of the local atomic environment effectively magnifies (3) the otherwise unobservable direct quadrupole radiation signal by a factor on the order of 10^{+6}, so that a direct electric signal may be observed by placing the sample between the plates of a capacitor.

In a previous experiment (3), *n*uclear *e*lectric *r*esonance *d*etection (NERD) was first demonstrated using the 30 MHz transition of ^{35}Cl in $NaClO_3$. In that experiment a small magnetic field was applied to remove the degeneracy of the $m = \pm 1/2, \pm 3/2$ states. The resulting mixed $m = \pm 1/2$ states allow the development of a detectable electric polarization FID signal after a single pulse. The electric signal was characterized by a beating of different $|\Delta m| = 1, 2$ transition frequencies between the mixed $m = \pm 1/2$ states and the $m = \pm 3/2$ states, distinguishable from the beat frequency signature produced by stray pickup of a direct nuclear magnetic signal at the same Larmor frequency. In GaAs the observation of a pure $|\Delta m| = 2$ transition from ^{75}As at the sharply tuned frequency 2ω is free of any nuclear magnetic signal at frequency ω. However, there is a small reactive signal pickup transient from the transmitter pulses at frequency ω.

In general the observation of a one-quantum or two-quantum electric signal requires that the expectation values

$$\langle I_{\pm}^2 \rangle, \langle I_z I_{\pm} + I_{\pm} I_z \rangle = \mathrm{Tr}\{\rho I_{\pm}^2\}, \mathrm{Tr}\{\rho(I_z I_{\pm} + I_{\pm} I_z)\} \quad (1)$$

be finite, which occurs only if the density matrix ρ is nonlinear in the nuclear spin operators. Thus in any system with equally spaced levels (including the degenerate NQR $^{35,37}Cl$ levels in $NaClO_3$), it is not possible to observe a NERD signal if the initial density matrix ρ is specified by a high temperature population distribution proportional to I_z, in which case the above traces of odd operators are zero. The requirement of a nonlinear ρ is met in the case of the zinc-blende structure, including GaAs and most other III–V semiconductors, by applying an external static electric field which produces a quadrupole shift due to the linear Stark effect (4). In the special case of $NaClO_3$ the electric FID signal is observed immediately after a single pulse because initial signals which beat with one another, associated with different frequencies, have different amplitudes, which is not the case for GaAs where a minimum of two RF pulses is required.

The NERD-induced polarization effect may be defined as the inverse of the linear Stark effect, where the former involves oscillating off-diagonal elements, and the latter involves on-diagonal elements which account for quadrupole frequency shifts. Both effects are expressed by the following Hamiltonian perturbation in dyadic form (3): with electric field gradients. The stick and ball description assumes that a nuclear quadrupole point source electric field induces polarization in nearest neighbor point atoms. This cannot account for the polarization spread over charge distributions and covalent bonds. Hence the definition of the "stick" distance is a vague one. Although one can only predict orders of magnitude of signal amplitudes by this approach, it is most valuable for predicting the signature and the sample orientation dependence of pulse transient signals which characterize the NERD phenomena.

A rough estimate of the NERD signal strength is obtained by expressing the local quadrupole electric field

$$H_Q = -\mathbf{P}_Q \cdot \mathbf{E} = -\mathbf{P}_E \cdot \mathbf{E}_Q \quad (2)$$

The macroscopic polarization induced by the precessing local quadrupole electric field $\mathbf{E}_Q$ is given

by $\mathbf{P}_Q = N\beta\overleftrightarrow{\alpha}\cdot \mathbf{E}_Q$, where $\overleftrightarrow{\alpha}$ is the atomic polarizability tensor. The Boltzmann factor β pertains to N participating quadrupole spins in the crystal. The electric field and corresponding oscillating voltage V on the capacitor plates are given by $V = (\mathbf{E}\cdot\hat{\mathbf{n}})d = 4\pi(\mathbf{P_Q}\cdot\hat{\mathbf{n}})d$, where $\hat{\mathbf{n}}$ is normal to the capacitor plate and d is the plate separation. The alternative form of H_Q, applicable to the dc linear Stark effect, defines $\mathbf{E}$ as the externally applied static electric field, where $\mathbf{P}_E = N\beta\alpha\mathbf{E}$ for an isotropic polarizability α. Here one views the applied electric field as inducing internal atomic dipole moments which interact with local nuclear quadrupole electric fields $\mathbf{E}_Q$.

The above model is a less rigorous equivalent of the usual analysis in terms of the quadrupole interaction as $E_Q = eQS/r_o^4$, where S = 25 is taken as the Sternheimer antishielding factor, the ^{75}As gyromagnetic ratio $\gamma = 0.73$ MHz/kG, $Q = 0.3 \cdot 10^{-24}$ cm^2, $\alpha = 10^{-24}$ cm^3 (assumed isotropic), $r_o = 1.2 \cdot 10^{-8}$ cm (estimated as one-half the As–Ga lattice distance, at the center of the covalent bond), and $N = 10^{22}$ cm^{-3}. Upon application of typical circuit parameters, scaled from the estimate given in detail in ref. (3), one obtains an approximate ratio of the ^{75}As NERD signal to the conventional magnetic NMR signal in the present experiment of about 1/10 to 1/100.

III. Experimental Results

The arrangement for a two-quantum NERD experiment consists of two independent resonant circuits: an RF transmitter coil tuned to frequency $\omega/2\pi$, inside of which is contained the sample, housed between two plates of a receiver capacitor tuned to frequency $2\omega/2\pi = 13$ MHz. The receiver is one used in a typical pulsed NMR system. For our measurements a single crystal of semi-insulating GaAs with dimensions $1.4 \times 1.4 \times 0.1$ cm^3 is placed with the (111) crystal planes parallel to the capacitor plates and transmitter coil axis. The circuits are cooled to 77 K to reduce noise and ensure high resistivity of the GaAs sample.

Applying the stick and ball model to the structure around an As atom shown in Figure 1, using isotropic polarizabilities for the four nearest neighbors, results in an induced polarization

$$P_{ind} = \frac{\alpha eQ}{r_o^4}\frac{5}{6}\sin^2\theta\left(\left\langle I_+^2\right\rangle + \left\langle I_-^2\right\rangle\right) \qquad (3)$$

for the (111) crystal orientation described above, where θ is the angle between the static polarizing magnetic field $\mathbf{H}_o$ and the Stark field $\mathbf{E}_o$. The polarization P_{ind} is summed over the spin ensemble to obtain the macroscopic polarization $\mathbf{P}_Q$ expressed in eqn. 2, which is proportional to the signal voltage V.

A DC electric field on the order of $|\mathbf{E}_o| = 20$ kV/cm is applied to the capacitor to provide the linear Stark shifts. The Stark-induced electric field gradient for this orientation is given by $eq = 2R|\mathbf{E}_o|/3$, where $R = 1.9 \times 10^{10}$ cm^{-1} is the linear Stark coefficient (4) for ^{75}As. The resulting quadrupole frequency shift is

$$\omega_q = \frac{eQRE_o}{2\hbar\sqrt{3}}\left(3\cos^2\theta - 1\right). \qquad (4)$$

The angle $\theta = 90°$ is chosen to provide the maximum NERD signal and an ω_q of the order of 7 kHz for the ^{75}As nuclei. Figure 1 shows the energy-level diagram and the NMR and NERD spectra for this system.

Figure 2 shows ^{75}As two-quantum FID and echo signals and the interference between them for a two pulse $90_x - \tau - 90_{\pm x}$ sequence. The inverses of all RF pulse widths exceed level broadening and electric Stark shifts. The second pulse alternates in phase by 180° from one two-pulse sequence to the next. The alternate data runs are added and subtracted from the signal average so that the nuclear signals add but the reactive pickup signals from the constant phase transmitter pulse cancel out. As the pulse spacing time τ is increased, the emergence of the electric quadrupole echo at $t=2\tau$ may be seen, although it is rapidly attenuated by dephasing due to magnetic inhomogenaeties and dipolar interactions.

The prediction of FID and echo signals may be carried out by use of the Majorana formula (5) to evaluate spin wave functions and expectation values, or a density matrix technique such as that devised by Bowden and Hutchison (6) may be used. Since the spin levels are broadened by both electric quadrupole and magnetic dipolar perturbations, we assume for simplicity that the broadenings due to these perturbations are independent of one another. The echo refocusing of electric strain inhomogeneous isochromats in this picture accounts for

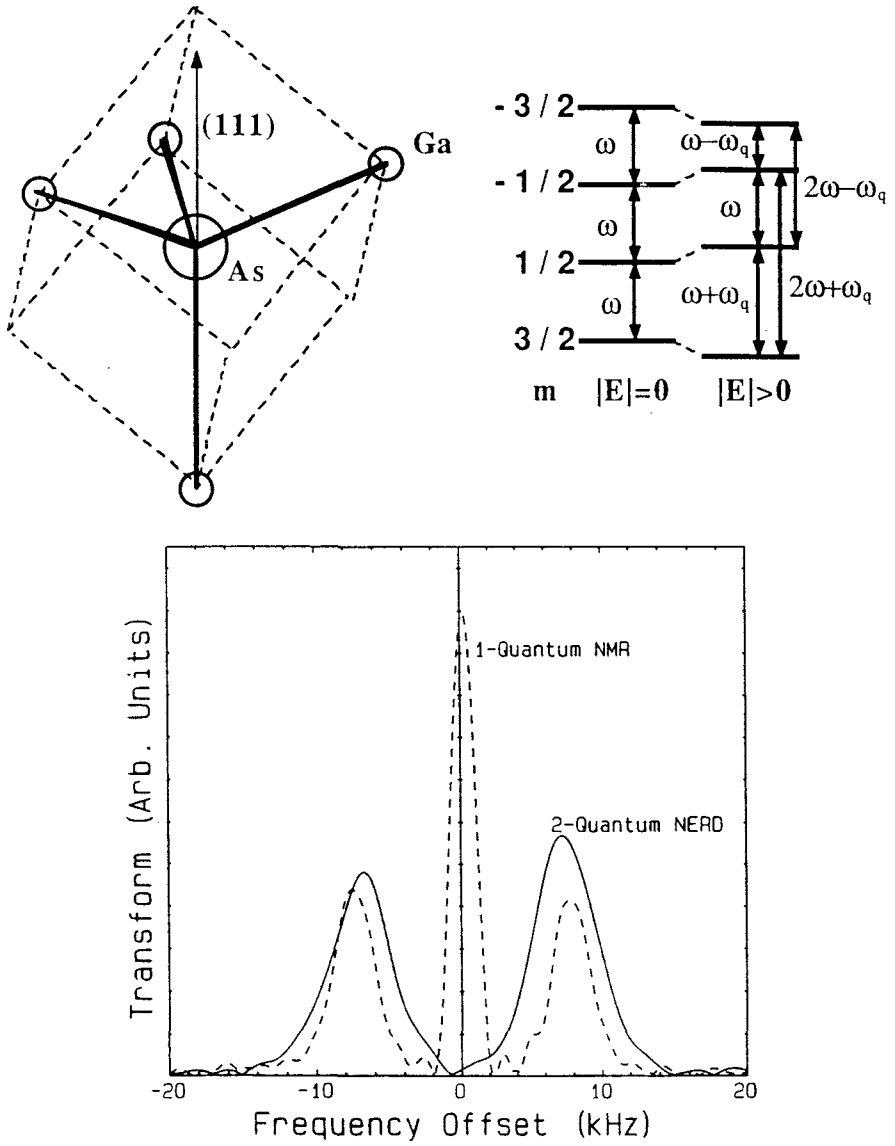

Figure 1: Tetrahedral structure of the four nearest neighbors in the zinc–blende structure, with the resulting energy-level diagram and NMR and NERD spectra for a spin I=3/2 nucleus subject to a Stark-induced quadrupole shift. In the bottom plot the dotted line shows the spectrum of a normal NMR experiment on Stark shifted ^{75}As in GaAs, while the solid line shows the spectrum of a two-quantum NERD experiment on the same sample.

observed NERD echo signals. As we are detecting a two-quantum coherence, the magnetic broadening isochromats do not refocus at the same time as the quadrupole interactions for a two pulse sequence. Therefore the NERD echo amplitude lifetimes T_{2e} remain very short, on the order of a millisecond, because of the defocusing caused by inhomogeneous and homogeneous magnetic broadening. The quadrupole echo is visible because the quadrupole dephasing time, $T^*_{2Q} \cong 50$ μs, is significantly less than the magnetic dephasing time, $T^*_{2M} \cong 200$ μs.

The dotted lines in Figure 2 are fits to the data according to this simple model of independent magnetic and quadrupolar broadening, where only the pulse separation time t is varied. The inverse of the quadrupole broadening of the system varied between $T^*_{2Q} \cong 40$ and 50 μs during the data runs because of progressive damage to the sample caused by the applied high voltage. We believe this damage is caused by the migration of charged defects or impurities, which over time produces changes in bulk strain and results in charge layers at the (111)

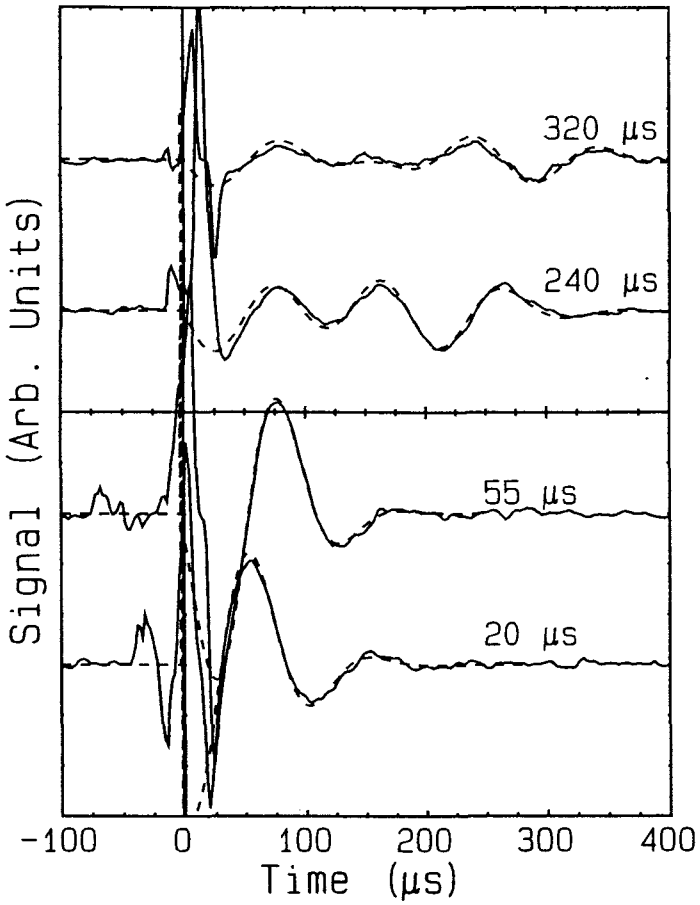

Figure 2: The detected two-quantum NERD signals following two 90° pulses. The time τ between the two pulses is shown for each run and the runs have been offset so the second pulse is at t = 0 on the horizontal axis. The dotted lines are fits to the experimental data, as described in the text.

surfaces. We have found that a fixed electric field ranging up to 1kV/cm caused by these charge layers opposes the applied field $\mathbf{E}_o$. This fixed field can be removed by warming the sample to room temperature for several hours, which then yields an increase of T^*_{2Q} to 80–90 μs.

A clearer measurement of the two-quantum NERD echo may be obtained by observing the echoes produced by a three pulse sequence, as this allows simultaneous or near-simultaneous refocusing of the magnetic and electric isochromats. For spin I = 3/2 nuclei the first two pulses generate one-, two-, and three-quantum coherences among the spin levels, and the third pulse in turn transfers these prepared coherences among the levels to provide observable two-quantum electric signals. Figure 3 shows two sets of data obtained from a $90_X - \tau_1 - 90_{\pm X} - \tau_2 - 90_X$ sequence. In the top trace $\tau_1 = 50$ μs, which is relatively short compared to the inhomogeneous dephasing time $T^*_{2Q} \cong 70$ μs. A portion of the two-quantum coherence seen as an FID following the second pulse is recreated after the third pulse as an echo at time $t \cong 2\tau_2 \cong 1$ μs. In this case both the electric and the magnetic isochromats refocus at approximately the same time. The bottom trace shows the multiple echoes formed by refocusing of the electric isochromats when $\tau_1 = 200$ μs and $\tau_2 = 600$ μs are both longer than T^*_{2Q}. We observe the three echoes labeled E1, E2, and E3 at times predicted by the inhomogeneous broadening model, but cannot achieve a reasonable fit to the signal amplitudes for the different echoes for these three pulse sequences.

IV. Conclusions

The direct detection of electric two-quantum coherence signals from an I = 3/2 spin system has been demonstrated without the need for an extra RF pulse to transfer unobservable two-quantum coherence to one-quantum coherence as required in

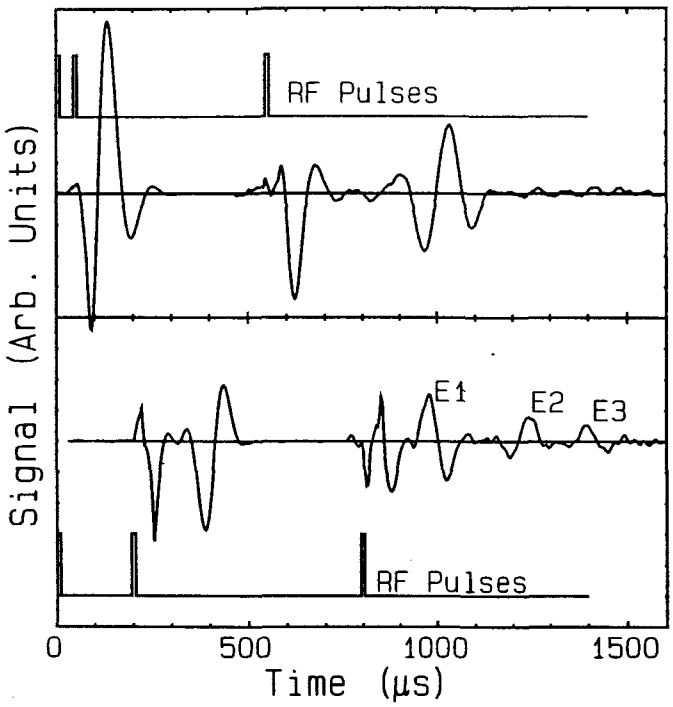

Figure 3: Two-quantum NERD FID and echo signals from three 90° x-axis pulses. Pulses are applied at t = 0, 50 and 550 μs for the top trace and t = 0, 200 and 800 μs for the bottom. The stronger signals after the second pulse in each trace are scaled down by a factor of five relative to the signals after the third pulse, and the lower trace is scaled up by a factor of two relative to the upper trace. Three quadrupole echoes, centered at t = 1000, 1200, and 1400 μs, labeled E1, E2, and E3, are visible in the bottom trace.

NMR multiquantum methods. The time evolution of the two-quantum coherence is mapped out in one "shot," whereas for NMR an additional inspection pulse must be applied for successive times in repeated pulse sequences to map out the two-quantum coherence.

Our echo analysis does not take into account the complicated magnetic dipolar echo-dephasing effects caused by the pulse reorientation of local dipolar fields. Many of the predicted echoes which occur following three pulses not only interfere with FID transients, but interfere among themselves if they are to be observed at all because the echo decay lifetimes are too short to always clearly resolve them. In some instances a predicted echo cannot be seen, or an echo predicted to be canceled out by the applied pulse sequence phase cycling is clearly visible. We do not understand this at present and hope to resolve it in a later report.

Given a fixed number of pulse excited spins over the entire spin spectrum, the initial FID amplitude of the electric polarization depends only upon the local distance and polarizability of atomic bonds and electrons in the vicinity of precessing nuclear quadrupole moments. On the other hand the initial FID signal in a conventional pulsed NMR experiment would be independent of these properties. One may conceive of experiments in which variations of these properties may be studied in terms of observed changes in the initial electric signal. Applications of external pressure, acoustic vibrations, and electric fields which induce charge layers in semiconductor structures or charge density waves in special systems are examples for future investigations.

Beyond the two-quantum case in NMR, an advanced and rigorous review of multiple quantum NMR spectroscopy techniques is provided in a highly comprehensive account (7) of modern NMR techniques by Ernst and co-authors. Under one cover, this account as a book includes descriptions of the important researches by Ernst and his collaborators at the ETH, Zurich which were recognized by the Nobel Prize.

V. Acknowledgments

We gratefully acknowledge helpful discussions with John Keltner, Larry Wald, and Charles Pennington and the support of the National Science Foundation.

VI. References

[1]C. P. Slichter, "Principles of Magnetic Resonance," 3rd ed., Chapter 9, Springer-Verlag, New York/Berlin 1990.

[2]M. Bloom and M. A. LeGros, *Can. J. Phys.* **64**, 1522 (1986).

[3]T. Sleator, E. L. Hahn, M. B. Heaney, C. Hilbert and J. Clarke, *Phys. Rev.* **B 38**, 8609 (1988).

[4]N. Bloembergen, in "Proceedings, X1 Colloque Ampere Conference on Electric and Magnetic Resonance, Eindthoven, 1962" (J. Smidt, Ed.), p. 39

North-Holland, Amsterdam,1963; F.A. Collins and N. Bloembergen, *J. Chem. Phys.* **40**, 3479 (1961).

[5]E. Majorana, Nuovo Cimento 9, 43 (1932); F. Bloch and I. I. Rabi, *Rev. Mod. Phys.* **17**, 237 (1945).

[6]G. J. Bowden and W. D. Hutchison, *J. Magn. Reson.* **67**, 403 (1966).

[7]R. R. Ernst, G. Bodenhausen and A. Wokaun, "Principles of Nuclear Magnetic Resonance in One and Two Dimension," Chapter 5, Clarendon Press, Oxford, 1990.